Journal of Power Technologies 101 (3) (2021) 154–162

A Duality of Biomagnetic fluid flow and heat transfer over a quadratic stretched sheet

M.G. Murtaza[1], E.E. Tzirtzilakis[1], and Mohammad Ferdows[3,✉]

[1]Department of Mathematics, Comilla, Cumilla-3506, Bangladesh
[2]Fluid Mechanics & Turbomachinery laboratory, Department of Mechanical Engineering, University of the Peloponnese, Patras, Greece
[3]Research group of Fluid Flow Modeling and Simulation, Department of Applied Mathematics, University of Dhaka, Dhaka-100
✉ferdowsmohammad@yahoo.com

Abstract

This paper investigates duality solutions of biomagnetic fluid flow and heat transfer over a permeable quadratically stretching/shrinking sheet in the presence of a magnetic dipole. The governing nonlinear partial differential equations are converted into a set of nonlinear ordinary differential equations with the help of suitable similarity transformations and then solved numerically by using the boundary value problem solver bvp4c built in MATLAB software. We examine the effects of a variety of pertinent parameters – the ferromagnetic parameter, suction parameter, stretching/shrinking parameter – on velocity and temperature profiles, as well as the skin friction coefficient and Nusselt number, which are presented graphically. Dual solutions exist for certain values of stretching/shrinking sheet and suction parameters. The skin friction coefficient data are evaluated and compared with previous published data and better agreement is achieved. Therefore, it can be said with confidence that our present analysis is accurate. It also shows that the ferromagnetic and stretched parameters result in reduced velocity and thereby influence the temperature profile.

Keywords: Biomagnetic fluid, FHD, Dual solution, Magnetic dipole, Quadratic stretching sheet.

1 Introduction

The main concept of biomagnetic fluid is the study of the interaction of biological fluids with an applied steady magnetic field whose flow is affected by the presence of a magnetic field. The composition of the biological fluid dictates the interaction of the fluid with the applied magnetic fields. All biological fluids may be considered biomagnetic fluids, because they contain ions that can interact with an applied magnetic field.

The study of biomagnetic fluid flow over a stretching sheet has many important applications in medical science and bio-engineering such as bio-sensing application, magnetic controlled drug delivery for the treatment of cancer and other pathological conditions, magnetic power generations and magnetic resonance imaging (MRI). Magnetic particles as carriers for therapeutic agents have been used in experimental animals and clinical applications in humans [1]; [2]; [3]; [4]; hyperthermia or hypothermia are used for various experimental medical techniques, such as cancer tumor treatment, injury treatment and open heart surgery [5]; [6].

The mathematical model of biomagnetic fluid was first introduced by [7]. An extended BFD mathematical model was developed by [8]. Numerical studies concerning basic flow configurations such as the BFD channel flow using the BFD model of [7] were investigated in [9]. The primary effect is the formation of a vortex in the area of application of the magnetic field. Similar basic flow configurations were also investigated in BFD flow problems considering non-Newtonian behavior of the biofluid [10]; [11]; [12]; [13]. [14]; [15] reported the flow analysis of biomagnetic fluid over a stretching sheet in the presence of a magnetic dipole.

On the other hand, numerous researchers analyzed the study of boundary layer flow over a quadratically stretching sheet. [16] analyzed the fluid flow past a permeable quadratically stretching/shrinking sheet. They employed the problem solver bvp4c built in MATLAB software to solve the equation and found that dual solutions exist. [17] investigated the two-dimensional stagnation-point flow and diffusion of chemically reactive species of a viscous and incompressible fluid past a permeable quadratically stretching/shrinking. [18] considered the case of mass diffusion of chemically reactive species under the influ-

ence of a magnetic field over a quadratic stretching sheet. [19] analyzed the dual solution of biomagnetic fluid over a nonlinear stretching/shrinking sheet using lie group analysis. [20] reported the existence of dual solutions of magneti-hydrodynamic fluid flow over a stretching/shrinking sheet. [21] reported the dual solutions existing for boundary layer flow and heat transfer over an exponentially stretching/shrinking sheet. It was reported by [22] that dual solutions exist for MHD flows over a shrinking surface. [23] investigated the dual solutions of MHD fluid flow and heat transfer over a nonlinear stretching/shrinking sheet with a convective boundary condition.

Motivated by the above studies, the present analysis considers the biomagnetic fluid flow and heat transfer past a permeable quadratically stretching/shrinking sheet. The partial governing equations are transformed into ordinary differential equations by using appropriate similarity variables, and then solved numerically using the boundary value problem solver, bvp4c, built in MATLAB software.

2 Mathematical Description

Consider a steady two-dimensional electrically non-conducting biomagnetic fluid flow and heat transfer of a viscous and incompressible fluid over an impermeable quadratically stretching/shrinking sheet as shown in Fig. 1, where x and y are the Cartesian coordinates measured along the surface and normal to it, the flow being at $y \geq 0$. It is assumed that the surface is stretched/shrunk in the x -direction with velocity $u_w\,(x)$ and it is also assumed that the velocity of the far flow is $u_e\,(x)$. Further, a magnetic dipole is located at a distance in such a way that its center lies exactly on the y-axis at distance b from the x-axis. The magnetic field points of the magnetic dipole are in the positive x-direction. It is also assumed that the surface temperature Tw and the ambient fluid temperature $T\infty$ are constants.

Under these assumptions the boundary layer equations are [24]

$$\frac{\delta u}{\delta\, x} + \frac{\delta v}{\delta\, y} = 0$$

$$u\frac{\delta u}{\delta\, x} + v\frac{\delta u}{\delta\, y} = u_e\frac{\delta u_e}{\delta\, x} + \frac{1}{\rho}\mu_0 M\frac{\delta H}{\delta x} + \frac{1}{\rho}\mu\left(\frac{\delta^2 v}{\delta x^2} + \frac{\delta^2 v}{\delta y^2}\right)$$

$$\rho c_p\left(u\frac{\delta T}{\delta\, x} + v\frac{\delta T}{\delta\, y}\right) + \mu_0 T\frac{\delta M}{\delta T}\left(u\frac{\delta H}{\delta\, x} + v\frac{\delta H}{\delta\, y}\right) = k\left(\frac{\delta^2 T}{\delta x^2} + \frac{\delta^2 T}{\delta y^2}\right)$$

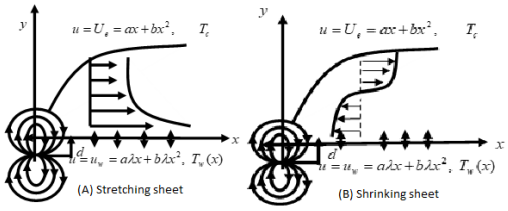

Figure 1: Geometry of the problem

The boundary conditions for the above mathematical model are given as [16]

$$u = u_w\,(x) = a\lambda x + b\lambda x^2, v(x) = v_w, T = T_w \quad at \quad y = 0$$

$$u = U_e\,(x) \to ax + bx^2,\ T \to T_c \quad as \quad y \to \infty$$

where u and v are the velocity components along the x and y axes, respectively, T is the fluid temperature, a is the thermal diffusivity, n is the kinematic viscosity and a and b are constants, with a > 0 . We note that λ is the stretching/shrinking parameter with $\lambda > 0$ for stretching and $\lambda < 0$ is for shrinking. We also note that when b $= 0$, it corresponds to the linearly stretching/shrinking sheet. The other case is b [?] 0, which corresponds to the quadratic stretching/shrinking sheet.

Magnetization parameter M is considered to be related to temperature T as [25]

$$M = K(T_c - T)$$

The magnetic dipole lies on the y-axis at distance d below the x-axis, which generates a magnetic field that is sufficiently strong to saturate the biofluid; $H_x,\ H_y$ are the components of the magnetic field $H = (H_x,\ H_y)$ given by [25]

$$H_x(x,y) = -\frac{\gamma}{2\pi}\frac{x^2 - (y+d)^2}{(x^2 + (y+d)^2)^2}$$

$$H_y(x,y) = -\frac{\gamma}{2\pi}\frac{2x(y+d)^2}{(x^2 + (y+d)^2)^2}$$

The magnitude $| H |= H$of the magnetic field is given by

$$H(x,y) = [H_x^2 + H_y^2]^{1/2} = \frac{\gamma}{2\pi}\left(\frac{1}{(y+d)^2} - \frac{1}{2}\frac{x^2}{(y+d)^4}\right)$$

3 Mathematical analysis

The mathematical analysis of the problem is simplified by introducing the following dimensionless coordinates [16]

$$\begin{gathered} X = x\sqrt{\frac{a}{\nu}}, \\ Y = y\sqrt{\frac{a}{\nu}}, \\ U = \frac{u}{\sqrt{a\nu}}, \\ V = \frac{v}{\sqrt{a\nu}}, \\ U_e = \frac{u_e}{\sqrt{a\nu}}, \\ \theta(\eta) = \frac{T_c - T}{T_c - T_w} \end{gathered}$$

By substituting (6) to (10) into equations (1) to (3), we get

$$\delta U \overline{\delta\ X + \frac{\delta V}{\delta\ Y} = 0}(1)$$

$$U\frac{\delta U}{\delta\ X} + V\frac{\delta U}{\delta\ Y} = U_e\frac{\delta U_e}{\delta\ X} + \left(\frac{\delta^2 V}{\delta X^2} + \frac{\delta^2 V}{\delta Y^2}\right) - \frac{2\beta X\theta}{(Y+\delta)^4}$$

$$\begin{gathered} \left(U\frac{\delta\theta}{\delta\ X} + V\frac{\delta\theta}{\delta\ Y}\right) + \\ \frac{1}{P_r}\beta\lambda_1(\epsilon - \theta)\left(\frac{2UX}{(Y+\delta)^4} - \frac{2V}{(Y+\delta)^3} + \frac{4X^2}{(Y+\delta)^5}\right) \\ = \frac{1}{P_r}\frac{\delta^2\theta}{\delta Y^2} \end{gathered}$$

Boundary conditions for the above mathematical model are given as [16]

$$u = U_w(x) = \lambda X + A\lambda X^2, v = V_w, \theta = 1 \qquad at\ Y = 0$$

$$u = U_e = X + AX^2, \theta = 1 \qquad at \quad Y \to \infty$$

Now we introduced the dimensionless variables [26], [16]

$$\psi = Xf(Y) + AX^2 g(y)$$

where ψ is the dimensionless stream function, which is defined in the usual way as $U = \frac{\delta\psi}{\delta Y}$and $V = -\frac{\delta\psi}{\delta X}$ so as to satisfy the continuity equation (9). Thus, we have

$$U = Xf'(Y) + AX^2 g'(Y)$$

and

$$V = -f(Y) - 2AXg(Y)$$

Substituting (17) and (18) into Eqs. (12) and (13), the following set of ordinary differential equations are obtained

$$f''' + ff'' - f'^2 + 1 - \frac{2\beta\theta}{(\eta+\alpha)^4} = 0$$

$$g''' - 3f'g' + 2gf'' + fg'' + 3 = 0$$

$$\theta'' + P_r f\theta' + \frac{2\lambda_a\beta(\theta - \epsilon)}{(\eta+\alpha)^3}f = 0$$

The corresponding transformed boundary conditions are

$$f'(0) = \lambda, f(0) = S, g(0) = 0, g'(0) = \lambda, \theta(0) = 1$$

$$f'(\infty) = 1, g'(\infty) = 1, \theta(\infty) = 0$$

The important physical characteristics skin friction coefficient C_f and the local Nusselt number Nu_x are described as

$$C_f = \frac{\tau_w}{\frac{1}{2}\rho u_w^2}$$

and

$$Nu_x = \frac{xq_w}{k(T_c - T_w)}$$

In Eqn. (24) and (25), τ_w is the shear stress at wall, while q_w represents the wall heat flux, defined by

$$q_w = -k\left(\frac{\delta T}{\delta y}\right)_{y=0}$$

$$\tau_w = \mu\left(\frac{\delta u}{\delta y}\right)_{y=0},$$

Introducing (26) and (27) into Eqn. (24) and (25), the skin friction coefficient and local Nusselt number can be written in dimensionless form as

$$\frac{1}{2}C_{fx}\sqrt{Re_x} = f''(0) + AXg''(0)$$

and

$$\frac{Nu_x}{\sqrt{Re_x}} = -\theta'(0)$$

where $Re_x = \frac{u_w(x)x}{\nu}$ is the local Reynolds number based on the stretching velocity $u_w(x)$.

4 Solution procedure

The systems of nonlinear ordinary differential equations (19) to (21) subject to boundary conditions (22) and (23) were solved numerically by using the boundary value problem solver, bvp4c function technique in MATLAB. To find the solution, the prerequisites are: (i) to reduce the system of higher order partial differential equations to a system of first order ordinary differential equations by introducing new variables,(ii) to write down the boundary conditions for the new variables, and (iii) to make appropriate initial guesses for the new variables.

Since the transformed governing equations are of third order, to reduce them into a system of first order ordinary differential equations, some new variables were defined as

$f = y_1, f' = y_2, f'' = y_3, g = y_4, g' = y_5, g'' = y_6, \theta = y_7, \theta' = y_8$

Thus, the two coupled higher order differential equations and the corresponding boundary conditions were transformed to a system of five first order ODEs along with new boundary conditions. The system of first order ODEs is:

$f' = y_2$

$y_2' = f'' = y_3$

$y_3' = -y_1y_3 + y_2^2 - 1 + \frac{2\beta y_7}{(\eta+\delta)^4}$

$g' = y_5$

$y_5' = g'' = y_6$

$y_6' = 3y_2y_5 - 2y_4y_3 - y_1y_6 - 3$

$\theta' = y_8$

$$y_8' = P_r y_1 y_8 - \frac{2\lambda_a\beta(\epsilon - y_7)y_1}{(\eta+\delta)^3}$$

subject to the initial boundary conditions:

$y_1(0) = S, y_2(0) = \lambda, y_5(0) = \lambda, y_4(0) = 0, y_7(0) = 1,$ when $\lambda < 1$, $y_2(\infty) = 0, y_5(\infty) = 0, y_7(\infty) = 0$

Equation (30) and Eq. (31) have been integrated numerically as an initial value problem to a given terminal point. All these simplifications had to be done for the purpose of using the MATLAB package. This program runs with a step size of $\eta = 0.01$ and then solved for the interval of $0 \leq \eta \leq \eta_\infty$ taking $\eta_\infty = 6$. This value was obtained by using the trial and error method.

5 Result and Discussion

For the purpose of computation we assumed that fluid blood with $\rho = 1050kg.m^{-3}$and $\mu = 3.2 \times 10^{-3}kgm^{-1}S^{-1}$,$\epsilon = 78.5$ and the viscous dissipation number 6.4×10^{-14}[14], $c_{p=}3.9 \times 10^3 Jkg^{-1}K^{-1}$ and $k = 0.5Jm^{-1}s^{-1}K^{-1}$ and hence $P_r = 25$ [15] . The values of β (which is related to the magnetic field) are assumed to be from 0 to 10 by [27] , where $\beta = 0$ corresponds to pure hydrodynamic flow. For validation of the numerical method, the numerical results for the skin friction coefficient (for a limiting case) are compared with those of [28]. The comparative study, presented in Table 1, shows that the results of the present investigation are in good agreement with those reported by [28].

Table 1. Comparison of skin friction coefficient for different values of stretching parameter with $\beta = 0$, s $= 0$, $P_r = 0.72$

Figs. 2 and 3 display the variations of the skin friction coefficients $(f''(0))$and rate of heat transfer $(\theta'(0))$with $\lambda < 0$ (shrinking sheet) and $\lambda > 0$(stretching sheet) for several values of ferromagnetic parameter β when $P_r = 21$, $S = 1$, $E = 78.5$. From figure 1 wit can be seen that the values of skin friction coefficient $f''(0)$ decrease as β increases. It can also be seen that dual solutions exist for a certain range of the shrinking parameter $\lambda < 0$. From this figure it appears that for $\beta = 5$ a unique solution exists for $\lambda > -0.2$ while dual solutions exist when $-1.565 < \lambda < -0.2$, no solution exists when $\lambda < \lambda_c$ where $\lambda_c = -1.565, -1.515, -1.465$, being the critical value of λ at which the two solution branches meet each other and thus a unique solution is obtained.

Fig. 3 shows the rate of heat transfer coefficient $\theta'(0)$ for different values of ferromagnetic parameter β with variation of the stretching/shrinking parameter λ. From the figure, it is observed that for the specified values of $\beta = 5$, the solution is unique when $\lambda > -0.25$ whereas dual solutions exist when $-1.575 < \lambda < -0.25$ and no solutions exist when $\lambda < -1.575$, where -1.575 is the critical value of λ and the

Table 1: Comparison of skin friction for different values of stretching parameter with $\beta = 0, S = 0, \mathrm{Pr} = 0.72$

value	Rosca et al.(2016)	Rosca et al.(2016)	present	present
lambda	1st solution	2nd solution	2nd solution	1st solution
0	1.2325877	—	—	1.232587
0.1	1.1465610	—	—	1.146560
0.2	1.0511300	—	—	1.051129
0.5	0.71323494	—	—	0.713295
1	0	—	—	0.00000
2	-1.88731	—	—	-1.887306
-0.25	1.4022408	—	—	1.402241
-0.5	1.4956698	—	—	1.495670
-0.75	1.4892983	—	—	1.489298
-0.25	1.4022408	—	—	1.402241
-0.5	1.4956698	—	—	1.495670
-0.75	1.4892983	—	—	1.489298
-1	1.3288170	—	—	1.328817
-1.1	1.186680	0.04922	0.04498	1.187016
-1.5	1.082800	0.11670	0.11323	1.082800
-1.2	0.932473	0.23365	0.23069	0.932473

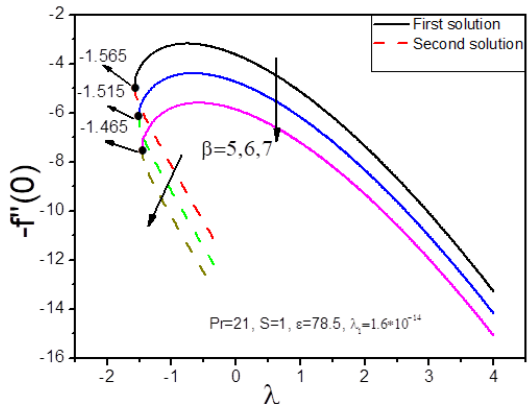

Figure 2: Variation of $f''(0)$ with $\lambda < 0$ (Shrinking sheet) and $\lambda > 0$ (Stretching sheet) for $\beta = 5, 6, 7$

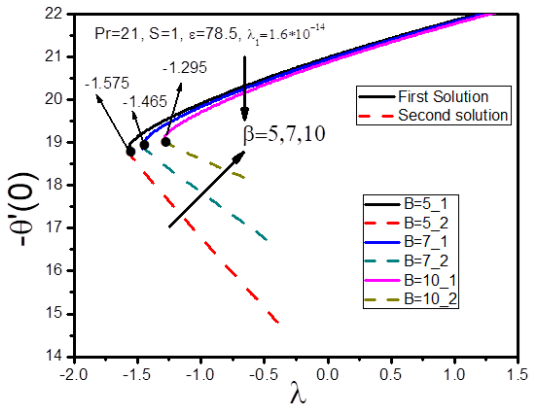

Figure 3: Variation of $-\theta'(0)$ with $\lambda < 0$ (Shrinking sheet) and $\lambda > 0$ (Stretching sheet) for $\beta = 5, 7,\ 10$

value of $\lambda_c = -1.575,\ -1.465,\ -1.295$ with specific values of $\beta = 5, 7, 10$. From this figure we also observe that the critical value λ_c decreases, as the value of the ferromagnetic parameter increases and that of the skin friction coefficient decreases. One may further observe that the effect of the ferromagnetic parameter diminishes in the range of λ for which a solution exists.

The variations of $f''(0)$ and $\theta'(0)$ with S for $\beta = 5, 7, 10$ are shown in Figs. 4 and 5 respectively. The values of S_c when $\beta = 5, 7, 10$ are $0.745,\ 0.805,\ 0.84500$ where S_c is the critical value of S at which the two solution branches meet each other and thus a unique solution is obtained. We also note that a dual solution exists for a specific range of values of the suction parameter.

From these figures, the following observations may be summarized for $\beta = 5$:

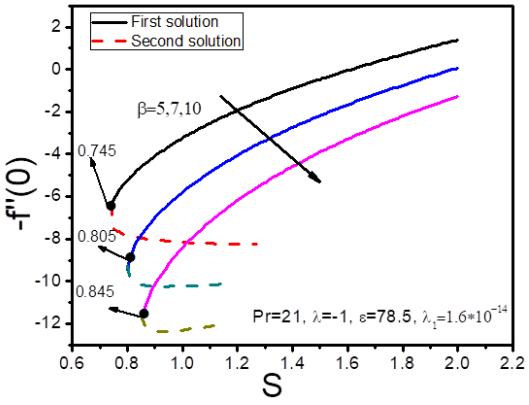

Figure 4: Variation of $f''(0)$ with S for $\beta = 5, 7, 10$

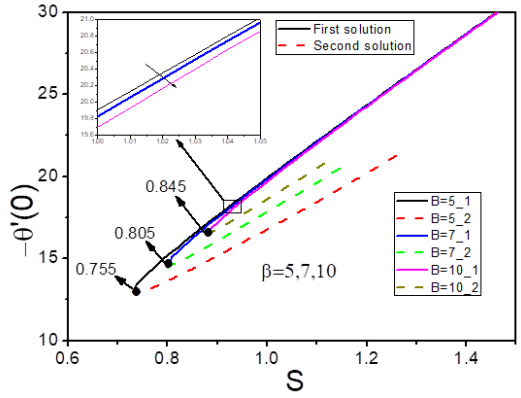

Figure 5: Variation of $-\theta'(0)$ with S for $\beta = 5, 7, 10$

(i) For $S < S_c < 1.3$ dual solutions exist.

(ii) When $S > 1.3$ the solution is unique.

(iii) For $S < S_c$ no solution exists.

It can also be shown that as the ferromagnetic parameter increases, both the skin friction coefficient and the heat transfer rate at the wall surface decrease where the value of the skin friction coefficient $f''(0)$ and heat transfer rate $\theta'(0)$ are increasing for the first solution as suction parameter S increases.

Figs. 6-8 illustrate the velocity profiles $f'(\eta)$ and $g'(\eta)$ and temperature distribution $\theta(\eta)$ for several values for $\beta = 1, 5, 10$ which satisfy the boundary condition (18) and (19) asymptotically. These figures reveal that although the biomagnetic fluid velocity $(f'(\eta))$ is reduced, fluid velocity $(g'(\eta))$is enhanced and temperature profiles $\theta(\eta)$ increased as the ferromagnetic parameter increases for the first solution, but for the second solution the velocity profile decreases near the sheet and reverse behavior is

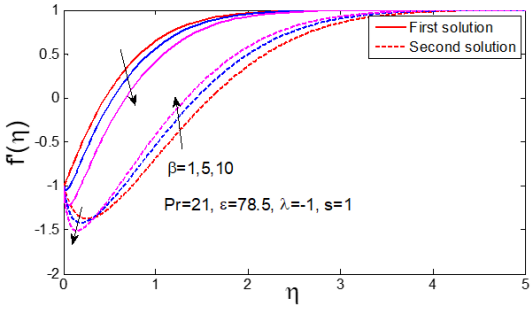

Figure 6: Dimensionless velocity profiles $f'(\eta)$ for several values for $\beta = 1, 5, 10$

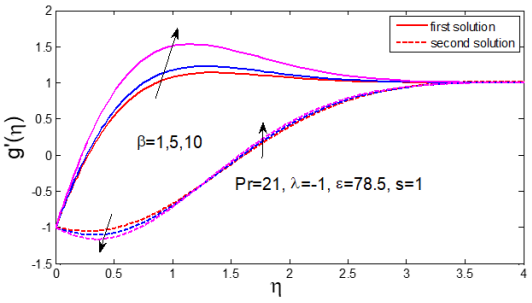

Figure 7: Dimensionless velocity profiles $g'(\eta)$ for several values for $\beta = 1, 5, 10$

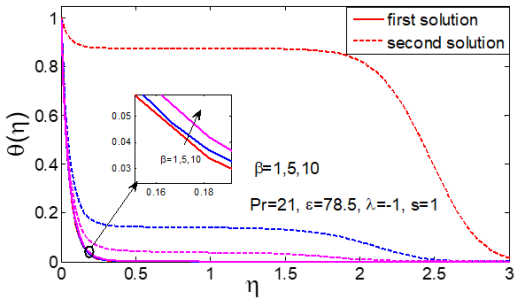

Figure 8: Dimensionless temperature profiles $\theta(\eta)$ for several values for $\beta = 1, 5, 10$

shown far away from the sheet. This happens because as the strength of the magnetic field characterized by beta β increases, the Kelvin force which opposes the flow in the boundary layer also increases and leads to enhanced deceleration of the flow and acceleration of the temperature distribution. The impact of the magnetic field on an electrically conducting biomagnetic fluid gives rise to a resistive-type force called Kelvin force which causes the flow motion to slow down and need more time, which gives more time for the heat to disintegrate to the flow while passing the sheet.

Figs. 9-11 display velocity $f'(\eta)$, $g'(\eta)$and temperature profiles $\theta(\eta)$for various values of the suc-

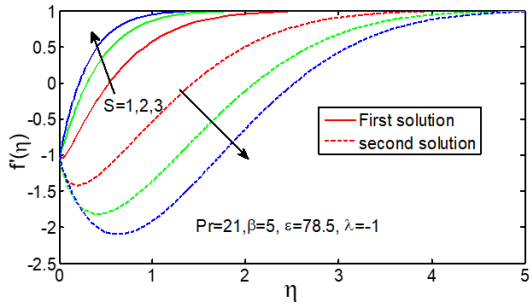

Figure 9: Dimensionless velocity profiles $f'(\eta)$ for several values for $s = 1, 2, 3$

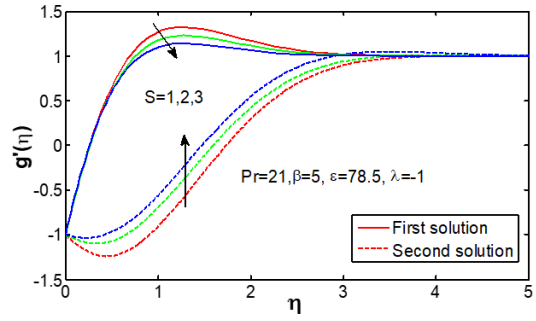

Figure 10: Dimensionless velocity profiles $g'(\eta)$ for several values for $s = 1, 2, 3$

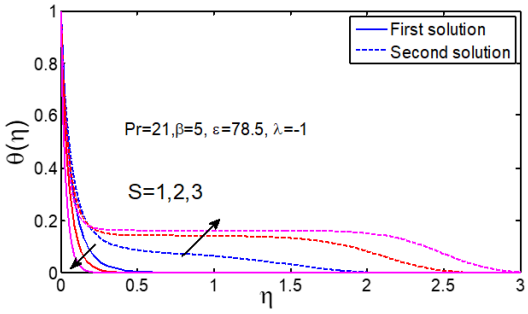

Figure 11: Dimensionless temperature profiles $\theta(\eta)$ for several values for $s = 1, 2, 3$

tion/injection parameter (S). Fig. 9 and 10 reveals that for the first solution, fluid velocity $f'(\eta)$ increases and velocity $g'(\eta)$decreases as the suction velocity enhances, while a reverse trend is observed in the case of the second solution. Physically it is realistic because of the suction effect near the wall. Fig. 11 demonstrates that the fluid temperature falls as the quantum of suction increases. The boundary layer thickness reduces as suction proceeds. However, this observation is valid only for the first solution. A reverse trend is found for the second solution. This observation implies that in the close vicinity of the surface, the thermal boundary layer thickness diminishes.

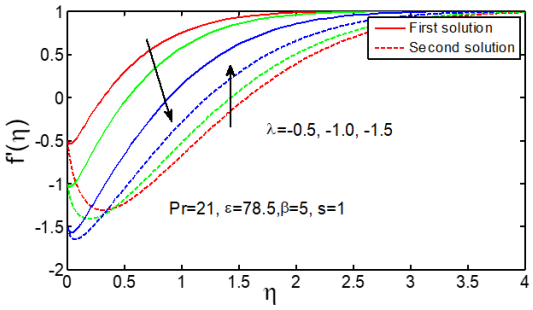

Figure 12: Dimensionless velocity profiles $f'(\eta)$ for several values for $\lambda = -0.5,\ -1.0,\ -1.5$

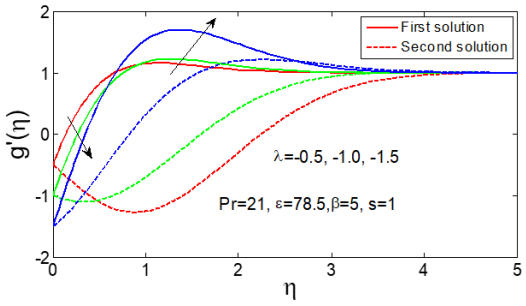

Figure 13: Dimensionless velocity profiles $g'(\eta)$ for several values for $\lambda = -0.5,\ -1.0,\ -1.5$

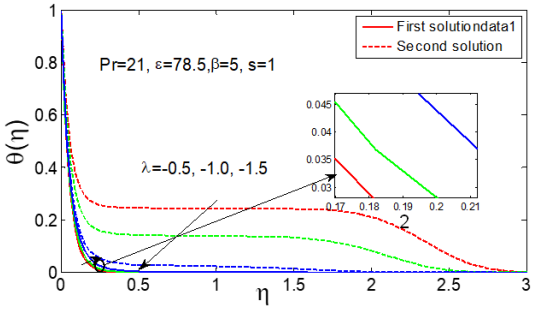

Figure 14: Dimensionless temperature profiles $\theta(\eta)$ for several values for $\lambda = -0.5,\ -1.0,\ -1.5$

The dimensionless velocity profiles ? ' (?), $g'(\eta)$and temperature profile $\theta(\eta)$ for several values of λ are demonstrated in Fig. 12 to 14. The dual velocity profiles of Figs. 12 and 13 show that velocity decreases with increasing magnitude of λ in the first solution and the converse result is shown for the second solution, i.e. the velocity increases. Physically it is realistic because the directions of straining and shrinking velocities are opposite. From Fig. 14, it can be seen that the values of $\theta(\eta)$ for the first branch solution decrease with increasing values of λ and the converse result is shown in the case of the second solution.

6 Conclusion and Summary

This paper investigated the duality analysis of biomagnetic fluid flow and heat transfer over a permeable quadratically stretching/shrinking sheet. The transformed governing equations are reduced to partial differential equations and solved numerically using the boundary value problem solver bvp4c built in MATLAB software.

The numerical values obtained for velocity and temperature as well as the skin friction coefficient and Nusselt number are presented graphically. The main results obtained in this research are as follows:

1. A unique solution exists for the stretching sheet while dual solutions exist for a particular range of shrinking sheet.
2. The critical value λ_c decreases as the value of the ferromagnetic parameter increases and that of the skin friction coefficient decreases.
3. Both the skin friction coefficient and the heat transfer rate at the wall surface decrease where the value of the skin friction coefficient $f''(0)$and heat transfer rate $\theta'(0)$are increasing for the first solution as the suction parameter S increases.
4. Biomagnetic fluid velocity $(f'(\eta))$is reduced, fluid velocity $(g'(\eta))$is induced and temperature profiles increased as the ferromagnetic parameter increases.
5. Fluid velocity $(f'(\eta))$ increases and velocity $(g'(\eta))$ decreases as the suction velocity enhances, while a reverse trend is observed in the case of the second solution.
6. The solution domain decreases as the suction parameter and stretching parameter with increasing ferromagnetic parameter.

References

1.Veiseh, M., Gabikian, P., Bahrami, S.B., Veiseh, O., and Zhang, et al., M. (2007) Tumor paint: a chlorotoxin: Cy5.5 bio conjugate for intraoperative visualization of cancer foci. *J Cancer Research*, **67**.

2.Glover, P. (2001) Limits to magnetic resonance microscopy. *J Reports on Progress in Physics*, **65**.

3.Kooi, M.E., Cappendijk, V.C., Cleutjens, K.B., Kessels, A.G., and Kitslaar, P.J.et al. (2003) Accumulation of ultra-smalls upper paramagnetic particles of iron oxide in human atherosclerotic plaques can be detected by in vivo magnetic resonance imaging. *J Circulation*, **107**.

4. (2004) .: In vivo detection of macrophages in human carotid atheroma-temporal dependence of ultrasmall super paramagnetic particles of iron oxide enhanced MRI. *J Stroke*, **35**.

5.Lin, W.L., Yen, J.Y., Chen, Y.Y., KW, J., and MJ, S. (1999) Relationship between acoustic aperture size and tumor conditions for external ultrasound hyperthermia. *Med. Phys*, **26**.

6.Stemme, O. (1998) *Magnetic wound treatment, in Magnetism in Medicine*, Wiley, Berlin.

7.Haik, Y., V, P., and J, C.C. (1999) *Biomagnetic fluid dynamics, in Fluid Dynamics at Interfaces*, Cambridge University Press.

8.Tzirtzilakis, E.E. (2005) A mathematical model for blood flow in magnetic field. *Phys Fluids*, **17**.

9.Loukopoulos, V., and E, T.E. (2004) Biomagnetic channel flow in spatially varying magnetic field. *Int J Eng Sci*, **42**.

10.Misra, J.C., and Shit, G.C. (2009) Biomagnetic viscoelastic fluid flow over a stretching sheet. *Appl Math Comput*, **210**.

11.Beg, O.A., Takhar, H.S., Bhargava, R., Sharma, S., and Hung, T.-K. (2007) Mathematical modeling of biomagnetic flow in a micropolar fluid-saturated Darcian porous medium. *Int J Fluid Mech Res*, **34**.

12.Beg, O.A., Bhargava, R., Rawat, S., Halim, K., and Takhar, H.S. (2008) Computational modelling of biomagnetic micropolar blood flow and heat transfer in a two-dimensional non-Darcian porous medium. *Meccanica*, **43**.

13.Misra, J.C., and Shit, G.C. (2009) Flow of a biomagnetic Visco– Elastic fluid in a channel with stretching walls. *Trans ASME J Appl Mech*, **76**.

14.Murtaza, M.G., Ferdows, M., Misra, J.C., and Tzirtzilakis, E.E. (2019) Three-dimensional biomagnetic Maxwell fluid flow over a stretching surface in presence of heat source/sink,. *International Journal of Biomathematics*, **12**.

15.Murtaza, M.G., Ferdows, M., and Tzirtzilakis, E.E. (2017) Effect of electrical conductivity and magnetization on the biomagnetic fluid flow over a stretching sheet. *Z. Angew. Math. Phys*, **68**.

16.Nasir, N.A.A.M., Ishak, A., and Pop, I. (2017) Stagnation-point flow and heat transfer past a permeable quadratically stretching/shrinking sheet. *Chinese Journal of Physics*, **55**.

17.Nazar, R., Arifin, N.M., Hafidzuddin, E.H., and Pop, I. (2015) Modelling of Stagnation-Point Flow and Diffusion of Chemically Reactive Species Past A

Permeable Quadratically Stretching/Shrinking Sheet. *International Conference on Modelling, Simulation and Applied Mathematics*.

18.Raptis, A., and Perdikis, C. (2006) Viscous Flow over a Nonlinearly Stretching Sheet in the Presence of a Chemical Reaction and Magnetic Field. *Int. J. Non-Linear Mech.*, **41**.

19.Ferdows, M., Murtaza, G.M., Misra, J.C., Tzirtzilakis, E.E., and Alsenafi, A. (2020) Dual solutions in biomagnetic fluid flow and heat transfer over a nonlinear stretching/shrinking sheet: application of lie group transformation method. *Mathematical Biosciences and Engineering Volume*, **17(5)**.

20.Naganthran, K., and Nazar, R. (2017) Dual Solutions of MHD Stagnation-point Flow and Heat Transfer past a Stretching/Shrinking Sheet in a Porous Medium. *4th International Conference on Mathematical Science AIP Conf.*.

21.Hafidzuddin, E.H., Nazar, R., Arifin, M., and Pop, I. (2016) Boundary layer flow and heat transfer over s permeable exponentially stretching/shrinking sheet with generalized slip velocity. *Journal of applied fluid mechanics,*, **9**.

22.Mahapatra, T.R., Nandy, S.K., and Pop, I. (2014) Dual solutions in magnetohydrodynamics stagnation point flow and heat transfer over a shrinking surface with partial slip,. *Journal of heat transfer, ASME*, **136**.

23.Dhanai, R., Ranaa, P., and Kumar, L. (2016) Multiple solutions in MHD flow and heat transfer of Sisko fluid containing nanoparticles migration with a convective boundary condition: Critical point. *The Eur. Phys. J. Plus,*, **131**.

24.Muhammad, N., Nadeem, S., and MT, M. (2018) Impact of magnetic dipole on a thermally stratified ferrofluid past a stretchable surface. *Proc IMechE Part E: J Process Mechanical Engineering*, **233**.

25.Murtaza, M.G., Tzirtzilakis, E.E., and Ferdows, M. (2018) Biomagnetic Fluid Flow Past a Stretching/Shrinking Sheet With Slip Conditions Using Lie Group Analysis. *8th BSME International Conference on Thermal Engineering AIP Conf. Proc.*.

26.Ziabakhsh, Z., Domairry, G., Bararnia, H., and H, B. (2010) Analytical solution of flow and diffusion of chemically reactive species over a nonlinearly stretching sheet immersed in a porous medium. *J. Taiwan Inst. Chem. Eng*, **41**.

27.Murtaza, M.G., Tzirtzilakis, E.E., and Ferdows, M. (2018) Numerical solution of three dimensional unsteady biomagnetic flow and heat transfer through stretching/shrinking sheet using temperature dependent magnetization. *Archives of mechanics*, **70**.

28.Rosca, A.V., Rosca, N.C., and Pop, I. (2016) Numerical simulation of the stagnation point flow past a permeable stretching/shrinking sheet with convective boundary condition and heat generation. *International Journal of Numerical Methods for Heat & Fluid Flow*, **26**.